THE JOURNAL OF BIOLOGICAL CHEMISTRY
Vol. 271, No. 42, Issue of October 18, pp. 26435–26442, 1996

Printed in U.S.A.

Cooperative Binding of DctD to the *dctA* Upstream Activation Sequence of *Rhizobium meliloti* Is Enhanced in a Constitutively Active Truncated Mutant*

(Received for publication, May 24, 1996, and in revised form, August 8, 1996)

Dean Scholl‡§ and B. Tracy Nixon‡¶

From the ‡Department of Biochemistry and Molecular Biology, The Pennsylvania State University, University Park, Pennsylvania 16802

DctD, a σ^{54}-dependent, two-component regulator, binds to promoter distal (A) and promoter proximal (B) sites in an activation sequence located upstream of the *dctA* promoter. We report gel filtration and quantitative DNase I footprint experiments supporting a model in which $DctD_2$ binds to these sites cooperatively. The global analysis of upstream activation sequences containing sites A and B, A and B one-half helical turn out of phase, and only B yielded values for the intrinsic and cooperative binding free energies of $\Delta G^0_A = -9.5 \pm 0.3$, $\Delta G^0_B = -11.2 \pm 0.2$, and $\Delta G^0_{AB} = -2.5 \pm 0.5$. A separate analysis of data from upstream activation sequences containing site A and a point mutant of site B, and site A and mutant site B one-half helical turn out of phase confirmed the estimate of cooperativity, yielding free energy values of $\Delta G^0_A = -9.4 \pm 0.2$, $\Delta G^0_{B(G\rightarrow C)} = -10.0 \pm 0.2$, and $\Delta G^0_{AB(G\rightarrow C)} = -2.2 \pm 0.4$. We previously showed that removing the two-component receiver domain from DctD, making $DctD_{\Delta(1-142)}$, yields a constitutively active truncated protein. Global analysis of binding data for $DctD_{\Delta(1-142)}$ showed that this constitutively active mutant has intrinsic binding energies equal to that of the inactive DctD protein, but that it displays significantly higher cooperativity ($\Delta G^0_A = -9.4 \pm 0.6$, $\Delta G^0_B = -11.1 \pm 0.3$, and $\Delta G^0_{AB} = -3.8 \pm 0.6$.).

Rhizobium meliloti are capable of utilizing C_4-dicarboxylates as the sole carbon and energy source. These compounds are believed to be provided by the host plants to fuel nitrogen fixation during symbiosis (1–5). Transport of dicarboxylates into the bacteria requires a single genetic locus containing the three genes *dctA*, *dctB*, and *dctD*. The *dctB* and *dctD* genes are transcribed divergently from *dctA*, which encodes a transport protein whose expression is increased in the presence of C_4-dicarboxylates (6–9). Transcription from the *dctA* promoter requires the alternate sigma factor, σ^{54} (10). In free living cells *dctB* and *dctD* are required for this increased expression, but in symbiotic bacteroids, *dctA* expression occurs at only somewhat reduced levels in the absence of *dctB* and *dctD* (11–13).

The *dctD* gene product, DctD, belongs to the σ^{54}-dependent activator sub-group of two-component response regulators. Two-component response regulators typically display homology in their NH_2-terminal 125 amino acids (6, 14, 15). These proteins are presumed to be phosphorylated at an aspartate located in the middle of this conserved region by histidine protein kinases, converting them from inactive forms to active ones (reviewed in Refs. 16 and 17). Like other σ^{54}-dependent transcriptional activators, but not all two-component response regulators, DctD also has a central domain that contains an ATP binding motif (6). ATP hydrolysis is required for DctD and other σ^{54}-dependent activators to catalyze the isomerization of closed complexes of the σ^{54}-form of RNA polymerase and promoter DNA to open ones (18, 19). Although the phosphorylated form of DctD has recently been demonstrated (20), it has not been studied in detail. It is known, however, that destabilizing or removing the NH_2-terminal two-component receiver module from DctD yields proteins which constitutively hydrolyze ATP and stimulate transcription (19, 21, 22). Both the inactive, wild type form of DctD and $DctD_{\Delta(1-142)}$, one such constitutively active mutant, have been physically cross-linked to σ^{54} and the β-subunit of RNA polymerase (23).

DctD also contains a third, COOH-terminal domain, which has a helix-turn-helix DNA binding motif. The protein binds with sequence specificity to an upstream activation sequence (UAS)[1] that is required for optimal transcription from *dctA* (Ref. 24; see Fig. 1). This UAS consists of two tandem dyad axes of symmetry termed the A (promoter distal) and the B (promoter proximal) sites that are separated by 33 base pairs. The A site is much less symmetric than the B site. From gel shift competition studies, it was inferred that the B site has a 50-fold higher affinity for DctD than the A site, and it was suggested that protein bound at both sites could interact cooperatively (25). Cooperative binding of a σ^{54}-dependent transcriptional activator to a UAS has been shown for NtrC in both *Escherichia coli* (26, 27) and *Salmonella typhimurium* (28). In the first report for *E. coli* NtrC, 27-fold cooperative binding was shown by filter binding assays, and it was concluded that phosphorylation of NtrC dramatically increased cooperativity by ~50,000-fold. For the *S. typhimurium* protein, gel shift assays were done using an artificial UAS that consisted of two identical high affinity sites; the results showed 20 ± 6-fold cooperativity for the unphosphorylated protein, which increased 12-fold to 230 ± 137 for phosphorylated NtrC. In a second study of *E. coli* NtrC (27), data from DNase I footprints was interpreted to support a 12-fold increase in cooperativity upon phosphorylation of NtrC. It has been suggested that cooperativity is needed to convert the NtrC protein from a transcriptionally inactive form to an active form (28, 29).

In this study we used DNase I footprinting experiments to

* This work was supported by National Institutes of Health Grant GM40404 (to B. T. N.). The costs of publication of this article were defrayed in part by the payment of page charges. This article must therefore be hereby marked "*advertisement*" in accordance with 18 U.S.C. Section 1734 solely to indicate this fact.

§ Current address: Agriculture and Agrifood Canada, Central Experiment Station, K. W. Neatby Building, Ottawa, Ontario K1A0C6, Canada.

¶ To whom correspondence should be addressed: Biochemistry and Molecular Biology, 327 S. Frear, The Pennsylvania State University, University Park, PA 16802. E-mail: btn1@psu.edu.

[1] The abbreviations used are: UAS, upstream activation sequence; PCR, polymerase chain reaction; bp, base pair(s).

measure the intrinsic and cooperative free energy contributions to binding of DctD and $DctD_{\Delta(1-142)}$ to the *dctA* UAS. Results show that the UAS is heterogeneous, with site A having less intrinsic affinity for DctD than site B, and that binding is cooperative. Moreover, the extent of cooperativity was significantly increased in the constitutively active mutant $DctD_{\Delta(1-142)}$ relative to that of the wild type protein. This increased cooperativity associated with the active state of truncated DctD is similar to the findings that phosphorylated NtrC has higher cooperativity than unphosphorylated NtrC, but it need not be caused by the same molecular mechanism.

EXPERIMENTAL PROCEDURES

DNA Biochemistry—Large scale DNA preparations were made by the alkaline lysis method (30). Small scale plasmid preparations were done by the boiling method (30). Transformations were done using calcium chloride to prepare competent cells. Preparation of single-strand M13 templates for sequencing was done according to the methods described in the Bio-Rad Mutagene kit. DNA sequencing was done using the Sequenase (U. S. Biochemical Corp.) kit. Restriction enzymes, DNA ligase, and Klenow DNA polymerase were purchased from Boehringer Mannheim. Nucleotides were obtained from Boehringer Mannheim and DuPont. Agarose was purchased from Life Technologies, Inc.; acrylamide and bisacrylamide were purchased from either Fisher or U. S. Biochemical Corp.

Purification of DctD—Plasmid pTRH1 was used to express wild type DctD in JM109 cells under control of the *lac* promoter (23). In this plasmid, the *dctD* gene together with a small portion of the upstream *dctB* gene was cloned into pBS (Stratagene). One to 4 liters of culture were grown in Luria Broth (1% tryptone; 0.0.5% yeast extract; 0.5% NaCl) supplemented with 50 μg/ml ampicillin at 30 °C until an optical density of 1.0 was reached, at which time isopropyl-1-thio-β-D-galactopyranoside was added to a final concentration of 1.0 mM and the culture was allowed to grow an additional 5–6 h. The cells were harvested by centrifugation and were resuspended in 20 mM Tris, 50 mM KCl, 5% glycerol, pH 7.9. The cells were then sonicated for 10 cycles of 30 s of disruption followed by 30 s of cooling using a Fisher model 300 Sonic Dismembrator. The solution was cleared by centrifugation at 12,000 rpm in a Sorvall SS-34 rotor for 40 min at 4 °C. Dry ammonium sulfate was added to the supernatant to a final concentration of 35% saturation, which was incubated for 30 min at 0 °C, and then centrifuged (12,000 rpm, 20 min, SS-34). The pellet was redissolved in the starting buffer, and dialyzed 1:1000 for 12 h at 4 °C against the starting buffer. The dialyzed solution was injected onto a 1.0-ml phosphocellulose (Sigma) column equilibrated with 20 mM Tris, 50 mM KCl, and 10% glycerol, at 4 °C. A linear gradient was run from 50 mM to 300 mM KCl over a volume of 25 ml. All chromatography in this work was done on a Pharmacia FPLC unit. Fractions between 150 mM and 250 mM KCl contained DctD protein, and they were pooled and concentrated against the starting buffer using Collodion Membranes (Schleicher & Schuell). DctD was estimated to be >95% pure by laser densitometry (Molecular Dynamics) and SDS-polyacrylamide gel electrophoresis (see Fig. 2*A*).

$DctD_{\Delta(1-142)}$ was purified essentially as described above, with the exception that 70 mM potassium thiocyanate was added to the starting buffer and dialysis buffer to help solubilize the protein (19). The phosphocellulose column did not contain thiocyanate, and the protein was concentrated against the same buffer as wild type DctD. Samples of both proteins were stored at −70 °C in 20 mM Tris, pH 7.9, 50 mM KCl, 10% glycerol. Protein concentrations were determined using the Bradford method (Bio-Rad). DNA binding activity remained stable over a period of several months.

Gel Filtration Chromatography—A 1 × 80-cm gel filtration column was packed with Superdex 200 (Pharmacia, prep grade) and was equilibrated with 20 mM Tris, 200 mM KCl, 5% glycerol, pH 7.9. The column was calibrated with Sigma molecular size markers (200, 150, 66, 29, and 12.4 kDa) according to the instructions by Sigma. Total volume loaded was 100 μl, and flow rate was 1 ml/min; slower flow rates did not improve resolution. DctD samples were incubated for 12 h after dilution prior to chromatography using a Pharmacia FPLC unit. All chromatography steps were performed at 5 °C. To measure amounts of protein that were below the level of UV detection, 1.5-ml fractions were collected from the column and were blotted onto Hybond-ECL nitrocellulose (Amersham) and were developed using the ECL chemiluminescence kit. Antibodies specific for DctD were purified from antiserum using protein-A affinity chromatography, as described previously (22). Developed blots were exposed to film and scanned using a laser densitometer (Molecular Dynamics) and the scans were quantified using ImageQuaNT software (Molecular Dynamics).

Construction of DNase I Templates—A 195-base pair fragment containing the *dctA* UAS but not its promoter was constructed using PCR. The region amplified was from base pairs −27 to −222 using plasmid pBG4 (22). The upstream primer contained a terminal *Bam*HI restriction site, while the downstream primer had a terminal *Eco*RI restriction site (all primers were purchased from Midland Scientific). Annealing was done at 60 °C, elongation at 72 °C, and denaturation at 94 °C. The reactions were done in a Perkin-Elmer Cetus DNA Thermal Cycler. The PCR product was electrophoresed on a 5% polyacrylamide gel, the proper size fragment was cut out of the gel, and DNA was eluted into TE (10 mM Tris, pH 8.0, 1 mM EDTA) and then precipitated with ethanol. The purified PCR product was then digested with *Bam*HI and *Eco*RI, extracted with phenol, precipitated with ethanol, and then ligated to pUC19. The ligation mix was used to transform MC1061, from which the resulting recombinant plasmid was purified using ultracentrifugation and CsCl. This created a construction in which the fragment could be labeled at either end by filling the 3′ end with [α-^{32}P]dATP. The *Bam*HI-*Eco*RI fragment was then subcloned into M13mp19 for site-directed mutagenesis, which was done using the Bio-Rad Mutagene *in vitro* mutagenesis kit. Fig. 1 shows the UAS constructions used in this study.

DNase I Footprinting—These experiments were conducted by using the quantitative DNase I footprint titration method essentially as described by others (31–33). End-labeled templates were made by first digesting 2–3 μg of the pUC constructs just described with *Bam*HI. The digested plasmid was then end-labeled by incubation with 1 mM dCTP, dTTP, and dGTP along with 10 μCi of [α-^{32}P]dATP and 1 unit of Klenow enzyme. It was then digested with *Eco*RI, and the mix was run on a 5% polyacrylamide gel. The appropriate band was cut out of the gel, and the DNA was allowed to elute into TE by shaking overnight and ethanol-precipitated at −70 °C. The radiolabeled DNA (~10 pM, 10,000 cpm) was allowed to bind to purified DctD or $DctD_{\Delta(1-142)}$ at 25 °C in 30 μl of binding buffer (20 mM Tris, pH 7.9, 50 mM KCl, 5% glycerol). No excess carrier DNA was added. Protein, diluted in binding buffer, was titrated over 7–8 log units with 3 concentration points/log. After 20 min, DNase I (Life Technologies, Inc.) was diluted appropriately (in 20 mM Tris, pH 7.6, 5 mM $MgCl_2$, 50 mM NaCl) and 10 μl was added to each binding reaction. The digestion was stopped after 30 s by adding 25 μl of 1% SDS, 10 mM EDTA, and the mix was then brought to 100 μl, supplemented with ammonium acetate and 1 μg of tRNA, and precipitated with ethanol. The precipitated DNA was allowed to dry under vacuum for at least 60 min, after which the samples were dissolved in sequencing stop solution and loaded onto a 6% denaturing polyacrylamide gel (0.5 × Tris-HCl/boric acid/EDTA electrophoresis buffer; Ref. 30). The gel was poured using a customized comb with 6-mm wells and 6 mm of space between the wells to fully separate material in adjacent lanes. The gels were dried after electrophoreses and were exposed to film.

After the film was developed and visualized, dried gels were cut in half (typically between lanes 12 and 13) and exposed for 40 min on a Betascope 603 Blot Analyzer (Betagen). The regions encompassing the A and B sites were each blocked off along with unoccupied regions above and below the sites (to be used as standards to normalize the data), and raw counts were collected within the regions. In every gel, a lane was run with no protein to be used as a control. Fractional protection for a given protein concentration was calculated using the formula given in Equation 1, where N is an experimental lane and R is the control lane with no protein added (31).

$$P = 1 - \frac{(\text{counts/min})_{N,\text{SITE}}/(\text{counts/min})_{N,\text{STD}}}{(\text{counts/min})_{R,\text{SITE}}/(\text{counts/min})_{R,\text{STD}}} \qquad \text{(Eq. 1)}$$

Numerical Analysis—The binding data were analyzed as described (32, 33) with the appropriate binding functions using nonlinear least-squares parameter estimation. These analyses were performed on a personal computer (486*i* CPU) using Lahey Fortran F77L (Lahey Computer Systems, Inc., Incline Village, NV) and NONLIN (Michael Johnson, University of Virginia, Charlottesville, VA), a fitting program that includes information about covariance in its error analysis (34). The reported 67% confidence limits are obtained by searching the N-dimensional parameter space for the variance ratio predicted by an F statistic. The method approximates the worst case joint confidence intervals and does not assume that the confidence limits are symmetrical about the optimal values.[2]

[2] The software is posted together with an explicit tutorial at the Internet site http://www.bmb.psu.edu/DNase1/.

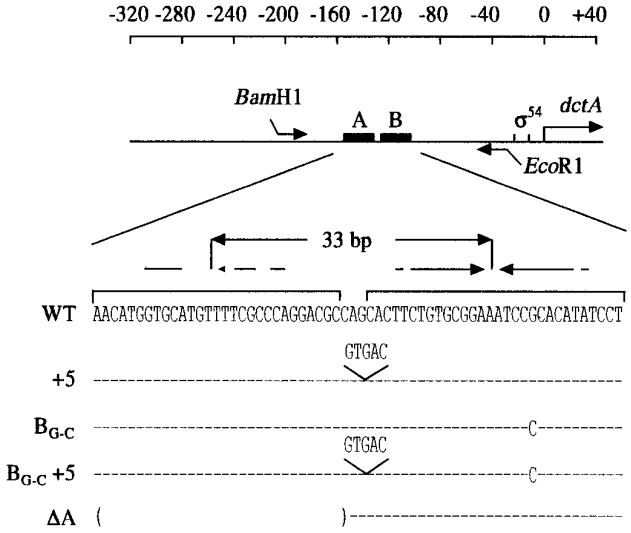

FIG. 1. **Mutant UAS templates used in this study.** The *dctA* promoter region is illustrated together with a 205-base pair fragment that was constructed using PCR. The promoter proximal primer had an *Eco*RI overhang, while the promoter distal primer had a *Bam*HI overhang. The fragment was then cloned into M13 for site-directed mutagenesis. The *arrows* above the sequence of site B indicate its nearly perfect dyad symmetry, which is broken for site A, especially for the leftmost half site. Also indicated are the bases of sites A and B that are protected from DNase I digestion by bound DctD (*brackets*), the 5-bp insertions, the G→C point mutation in site B, and the bases removed in deleting site A.

The intrinsic binding and cooperativity parameters that describe protein-DNA binding interactions are highly correlated. These parameters can only be resolved by simultaneous analysis of multiple experiments that are linked by common fitting parameters (33, 35). The five parameters of Table I were thus resolved by simultaneous analysis of various combinations of duplicate experiments for the five DNA templates shown in Fig. 1. All data points were given equal weight in the analyses. As shown in the figure, mutants were constructed in which: 1) a 5-bp insertion was placed between sites A and B; 2) site A was deleted; 3) a 1-bp substitution was introduced to site B; and 4) site A and mutant site B were separated by a 5-bp insertion. Titrations of sites that were separated by one-half helical turn on a single DNA template were treated as if they were from two separate, reduced valency templates. Data for DNA templates containing the B site point mutant were analyzed with the assumption that the intrinsic binding to site A remains unchanged by the point mutation in site B. The analysis did allow for the point mutation in site B to change the cooperativity, however, by treating it as a separate parameter distinct from that of the wild type template (see Table I). The fractional probabilities of the UAS configurations are given by Equation 2.

$$f_s = \frac{e^{\frac{-\Delta G_s}{RT}}[\mathrm{L}]^j}{\sum_s e^{\frac{-\Delta G_s}{RT}}[\mathrm{L}]^j} \qquad \text{(Eq. 2)}$$

ΔG_s is the free energy contributions for configuration s, R is the gas constant, T is the absolute temperature, [L] is the concentration of free protein ligand, and j is the number of ligands bound to configuration s. The free energies are related to the corresponding microscopic equilibrium constants k_i by the relationship shown in Equation 3.

$$\Delta G = -RT\ln k_i \qquad \text{(Eq. 3)}$$

The equation for fractional occupancy of a given site on a given template is obtained by adding the fractional probabilities for all states existing for that template in which the given site is occupied. Fractional occupancy at sites A and B on a wild type template are thus as shown in Equations 4 and 5.

$$Y_A = f_2 + f_5 \qquad \text{(Eq. 4)}$$

$$Y_B = f_3 + f_5 \qquad \text{(Eq. 5)}$$

For the template with the point mutation in site B, they are given by Equations 6 and 7.

$$Y_A = f_2 + f_6 \qquad \text{(Eq. 6)}$$

$$Y_{B_{G\to C}} = f_4 + f_6 \qquad \text{(Eq. 7)}$$

Occupancies at sites A, B, and $B_{G\to C}$ on the 5-bp insertion or A site deletion templates are shown in Equations 8–10.

$$Y_A = f_2 \qquad \text{(Eq. 8)}$$

$$Y_B = f_3 \qquad \text{(Eq. 9)}$$

$$Y_{B_{G\to C}} = f_4 \qquad \text{(Eq. 10)}$$

Fractional protection from DNase I is directly proportional to fractional occupancy, but even saturating concentrations of protein do not completely protect from DNase I. For this reason, the final equation used in fitting the protection data (P) and the appropriate fractional occupancy function (Y) was as given in Equation 11.

$$P = (U - L) \times Y + L \qquad \text{(Eq. 11)}$$

U is the upper limit of protection, and L is the lower limit of protection. A concentration range of at least 7 orders of magnitude was used in each titration to aid in estimating the transition end point parameters. For calculating protein concentration, DctD was considered to be a dimer (see results) present in excess of DNA, and protein preparations were assumed to be 100% active. Gel shift experiments showed that ≥99% of each of the labeled DNA fragments was bindable.

RESULTS

Purification of DctD—Purification of *R. meliloti* DctD from an overexpression strain was accomplished in a three-step procedure starting with a sonication of cells to generate a crude extract, followed by a 35% ammonium sulfate precipitation, and finally elution from a phosphocellulose column using a KCl gradient. This purification procedure is similar to the procedure described for purification of $DctD_{\Delta(1-142)}$ (19), with the exception that wild type DctD seems to be more soluble than the truncated mutant and does not require potassium thiocyanate or deoxycholate to prevent it from precipitation. Fig. 2*A* shows material from one such purification separated on an SDS-polyacrylamide gel. For all preparations used in this study, 95–98% purity was obtained from the phosphocellulose chromatography.

DctD Is a Homodimer—Small zone gel filtration experiments indicated that at 2.3 μM concentrations, DctD emerged from the column in a single peak at 90-ml elution volume (Fig. 2*B*). For this column, a 90-ml elution volume was typical of proteins with a molecular mass of 120,000 daltons. Since the predicted monomer size for DctD is 56,000, we propose that the protein is a homodimer at this concentration. To determine if a shift in the equilibrium concentrations of monomer and dimer occurs over concentrations relevant to the DNA binding studies reported here, we ran samples on the gel filtration column at concentrations down to 2.3 nM monomer. To detect these low amounts of protein, fractions were collected and immunoblotted to find the elution volume of the protein. As can be seen in Fig. 2*B*, neither the elution volume nor the shape of the peak changed between ~1 nM and ~1 μM concentrations of $DctD_2$.

$DctD_2$ Binds the dctA UAS Cooperatively—We used DNase I footprinting to measure fractional occupancy of $DctD_2$ at the *dctA*-UAS, and at two mutant forms designed to serve as "reduced-valency" templates (see Fig. 1). First, a 5-base insertion was placed between the two sites orienting them on opposite faces of the DNA helix, which in theory eliminates any protein-protein interaction between molecules bound at the two sites. Second, an A site deletion construct was made so that $DctD_2$ can only occupy the B site. The data from two independent repetitions of each experiment were then analyzed by global, nonlinear regression to extract estimates for the intrinsic binding and cooperativity free energies (Table II, row 1) as well as

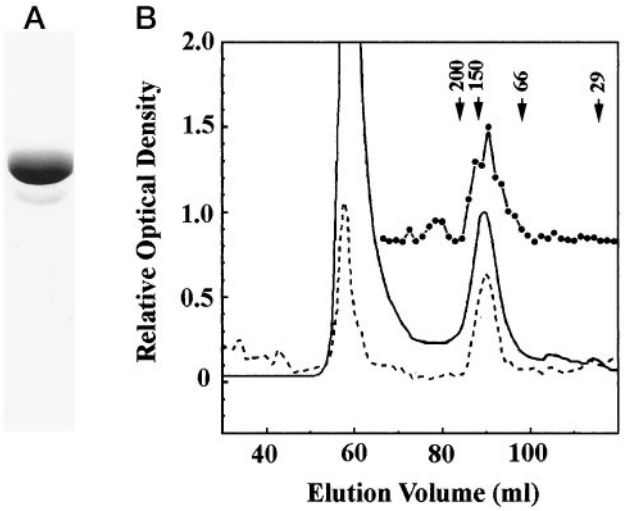

FIG. 2. **Purified DctD has a molecular mass of 120,000 daltons.** *A*, proteins in a DctD preparation were separated on an SDS-polyacrylamide gel and stained with Coomassie Blue. *B*, elution profiles of gel filtration studies. $UV_{280\ nm}$ absorption tracings are shown for DctD run at total monomer concentrations of 2.3 μM (*solid line*) and 230 nM (*dashed line*). The peak at 58 ml elution volume is for blue dextran, marking the void volume for the column. Separate runs (data not shown) showed no material in the void volume when only DctD was run. The top elution profile (*filled circles*) represents the immunodetected material from a sample loaded at 2.3 nM total monomer concentration. The *arrows* indicate elution volumes of protein standards. Note that the elution volumes are identical in all cases indicating that DctD is in the same multimeric state at concentrations relevant to this study, probably existing as a dimer.

the upper and lower protection limits for each titration (data not shown). The estimated parameter values were used to recast the observed fractional protection data as fractional occupancies, which were then plotted as the familiar binding isotherms for the wild type template (Fig. 3*A*), for the insertion template (Fig. 3*B*), and for the site A deletion mutant (Fig. 3*C*). The results suggest that sites A and B have different intrinsic affinities, and that binding to these two sites is cooperative. For the wild type template, the binding isotherms overlapped for both the A and B sites. In the case of the insertion mutant, however, occupancies were lower than for the wild type DNA, with site A showing considerably less affinity than site B. The site A deletion mutant showed only occupancy at the B site. The square root of the variance for the global analysis was 0.053, and the residuals between the observed data and the model, plotted below the isotherms in Fig. 3, were typically less than $\pm$ 0.2.

Analyses of the data for each DNA template and all other combinations of them are also shown in Table II. Combining the data sets for wild type and 5-bp insertion templates provided enough information for the analysis to converge on estimates of intrinsic binding and cooperativity that were essentially identical to those of the complete combination. Removing the information about binding to site A by combining data from wild type and site A deletion templates, or just considering the data from the wild type template, however, resulted in replacing most of the cooperativity energy with increased intrinsic binding to site A. For these data sets, holding either the cooperativity or site A intrinsic binding free energies constant restored the corresponding estimate to values derived in the more complete analyses. Analyses of the site A deletion and 5-bp insertion templates together or singly yielded parameter estimates that were very consistent with those of the global analysis. The square roots of the variances for all of these analyses were between 0.060 and 0.046.

To provide a different context for measuring the free energy of cooperativity and intrinsic binding to site A, a point mutation was introduced in the B site, making $B_{G\rightarrow C}$, and the corresponding 5-bp insertion mutation was also constructed (see Fig. 1). The specific point mutation chosen was the most

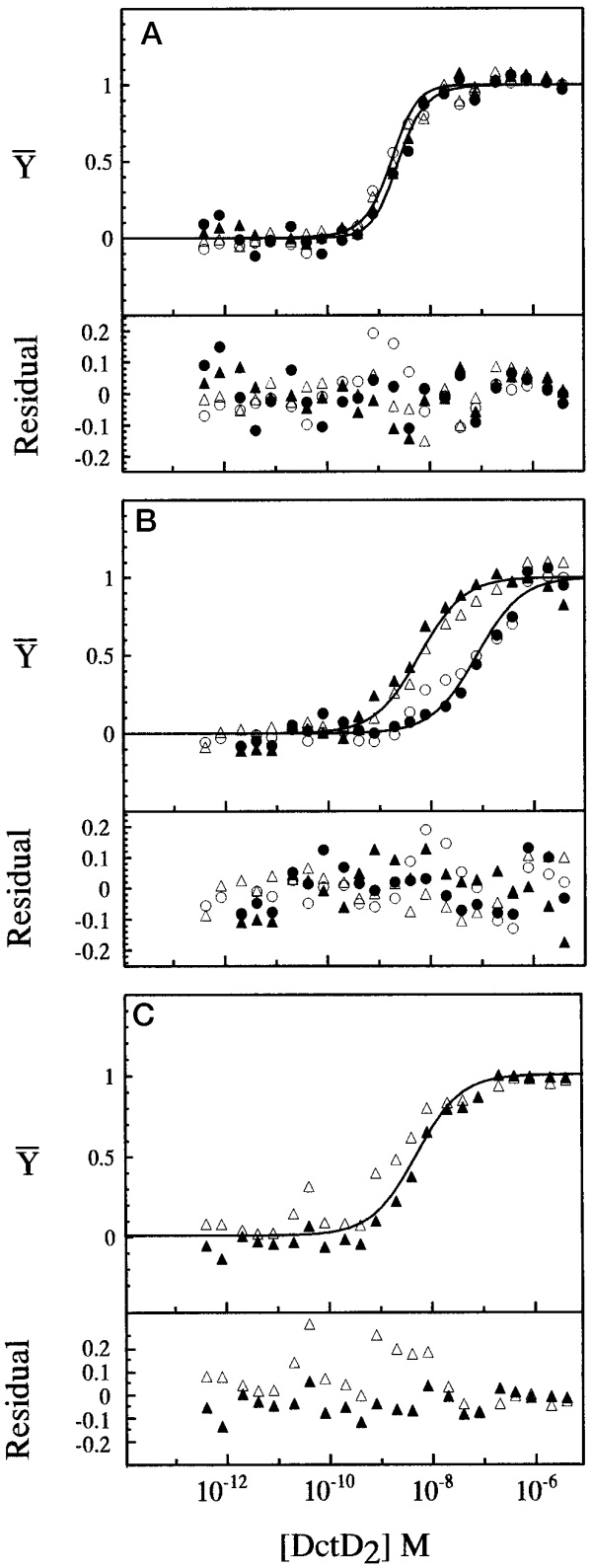

FIG. 3. **$DctD_2$ binding curves derived from DNase I footprint titrations of WT, +5, and ΔA templates.** *Open* and *closed symbols* represent different experiments. *Circles*, site A; *triangles*, site B. *A*, wild type template; note that the A and B sites are both occupied at the same DctD concentrations. *B*, 5-base pair insertion template. *C*, site A deletion template; note that occupancy at the B site is identical with the B site isotherms in the 5-base pair insertion mutant.

TABLE I

DNA configurations and associated free energy states for $DctD_2$ binding to the wild type and mutant dctA UAS elements

Binding sites are denoted as vacant (O) or occupied by DctD dimer (D_2). Cooperativity interactions are denoted by ↔. The total Gibbs free energy of each configuration is given as the sum of contributions from five free energy terms. ΔG_A, ΔG_B, and $\Delta G_{B(G\rightarrow C)}$ are the intrinsic free energies for binding to the corresponding sites; ΔG_{AB} and $\Delta G_{AB(G\rightarrow C)}$ are the free energies of cooperative interactions between liganded sites in the wild type and mutant UAS constructs, respectively.

State	DNA configuration					Gibbs free energy
	Site B		Site A		Site $B_{G\rightarrow C}$	
1	O		O		O	Reference state
2	O		D_2		O	ΔG_A
3	D_2		O		O	ΔG_B
4	O		O		D_2	$\Delta G_{B(G\rightarrow C)}$
5	D_2	↔	D_2		O	$\Delta G_A + \Delta G_B + \Delta G_{AB}$
6	O		D_2	↔	D_2	$\Delta G_A + \Delta G_{B(G\rightarrow C)} + \Delta G_{AB(G\rightarrow C)}$

TABLE II

Microscopic Gibbs free energies of $DctD_2$-UAS interactions resolved by footprint titration of wild type and mutant UAS elements

Free energies (in kilocalories per mole) are presented with 67% confidence intervals according the two-site cooperativity model. Values in parentheses were fixed for that analysis. WT, wild type.

UAS elements	ΔG_A	ΔG_B	ΔG_{AB}	$\Delta G_{B(G\rightarrow C)}$	$\Delta G_{AB(G\rightarrow C)}$	σ^a
WT, +5, Δ*A*	−9.5 ± 0.3	−11.2 ± 0.2	−2.5 ± 0.5			0.053
WT, +5	−9.5 ± 0.3	−11.1 ± 0.2	−2.6 ± 0.5			0.050
WT, Δ*A*	−11.2 ± 0.4	−11.3 ± 0.1	−0.7 ± 0.6			0.051
	−9.5 ± 0.2	−11.2 ± 0.2	(−2.5)			0.054
	(−9.5)	−11.2 ± 0.2	−2.5 ± 0.5			0.054
WT	−11.2 ± 0.4	−11.3 ± 0.3	−0.7 ± 0.7			0.046
WT	−9.8 ± 0.5	−10.9 ± 0.5	(−2.5)			0.050
+5, Δ*A*	−9.5 ± 0.4	−11.2 ± 0.2				0.054
+5	−9.5 ± 0.3					0.052
+5		−11.1 ± 0.2				0.049
Δ*A*		−11.3 ± 0.2				0.060
$B_{G\rightarrow C}$, $B_{G\rightarrow C}$ +5	−9.4 ± 0.2			−10.0 ± 0.2	−2.2 ± 0.4	0.049
$B_{G\rightarrow C}$	−10.7 ± 0.3			−10.4 ± 0.4	−0.4 ± 0.06	0.044
$B_{G\rightarrow C}$	−10.4 ± 0.4			−8.9 ± 0.4	(−2.2)	0.049
$B_{G\rightarrow C}$ +5	−9.3 ± 0.2					0.041
$B_{G\rightarrow C}$ +5				10.0 ± 0.2		0.041
WT, +5, Δ*A*, $B_{G\rightarrow C}$, $B_{G\rightarrow C}$ +5	−9.4 ± 0.3	−11.2 ± 0.2	−2.7 ± 0.4	−10.0 ± 0.2	−2.2 ± 0.4	0.052

[a] Square root of the variance of the fitted curves.

deleterious one of a set of mutations previously shown to reduce UAS function *in vivo* (25). The parameter values estimated by global nonlinear regression analysis of the combined data from these two templates (Table II) were used to determine the corresponding binding isotherms (Fig. 4, *A* and *B*). The values are consistent with the mutation in site B reducing the intrinsic affinity for $DctD_2$ by 1.2 kcal/mol, but leaving unaltered the binding to site A and the cooperativity between the protein-DNA complexes. Separate analysis of data from the point mutant template failed to detect cooperativity; instead, this analysis yielded increased intrinsic binding to site A. Moreover, fixing cooperativity at −2.2 kcal/mol in the separate analysis yielded values for intrinsic binding that were increased for site A and decreased for site B, compared to those estimated for the combined data. Separate analysis of data from the 5-bp insertion template yielded values consistent with the combined analysis. The square root of the variances of fit for these analyses were between 0.041 and 0.049. The data from these two templates were also combined with that of the previously discussed templates. The global analysis of all five templates yielded results that were in excellent agreement with the prior analyses (Table II).

The Truncated, Constitutively Active Mutant $DctD_{\Delta(1-142)}$ Displays More Cooperativity than DctD—We have previously characterized a truncated DctD mutant, $DctD_{\Delta(1-142)}$, which lacks the NH_2-terminal 142 residues of the wild type protein. Unlike DctD, $DctD_{\Delta(1-142)}$ is not regulated by the two-component receiver function, and it is constitutive for both transcriptional activation and the required ATP hydrolysis (19). To some extent, $DctD_{\Delta(1-142)}$ thus represents the activated state of DctD. The UAS-binding properties for $DctD_{\Delta(1-142)}$ were determined using the wild type and the 5-bp insertion templates to assess potential differences between the states of active and inactive activator (Table III and Fig. 4*C*). The data were analyzed assuming that $DctD_{\Delta(1-142)}$ also exists in a single state of dimer over the concentrations tested. The global analysis yielded Gibbs free energies for intrinsic binding to sites A and B that were indistinguishable from those of wild type protein; however, the estimate of cooperativity free energy was significantly elevated from −2.7 ± 0.4 kcal/mol for wild type protein to −3.8 ± 0.6 kcal/mol for the truncated protein. Separate analysis of the data for the wild type UAS converged upon a consistent set of parameter estimates, but the confidence intervals were very large and asymmetric. Fixing the cooperativity parameter at −3.8 kcal/mol yielded estimates of intrinsic binding free energies that were consistent with the global analysis, but these estimates still had rather large errors. Separate analysis of the data from the UAS bearing a 5-bp insertion between sites yielded estimates in excellent agreement with those of the combined analysis. The square root of the variances of fit for these analyses were between 0.46 and 0.69.

DISCUSSION

The results reported here confirm that $DctD_2$ binds specifically to DNA at two sites that make up the *dctA* upstream activation sequence. They also confirm that the intrinsic affinity of $DctD_2$ is ~20-fold lower for the A site than for the B site.

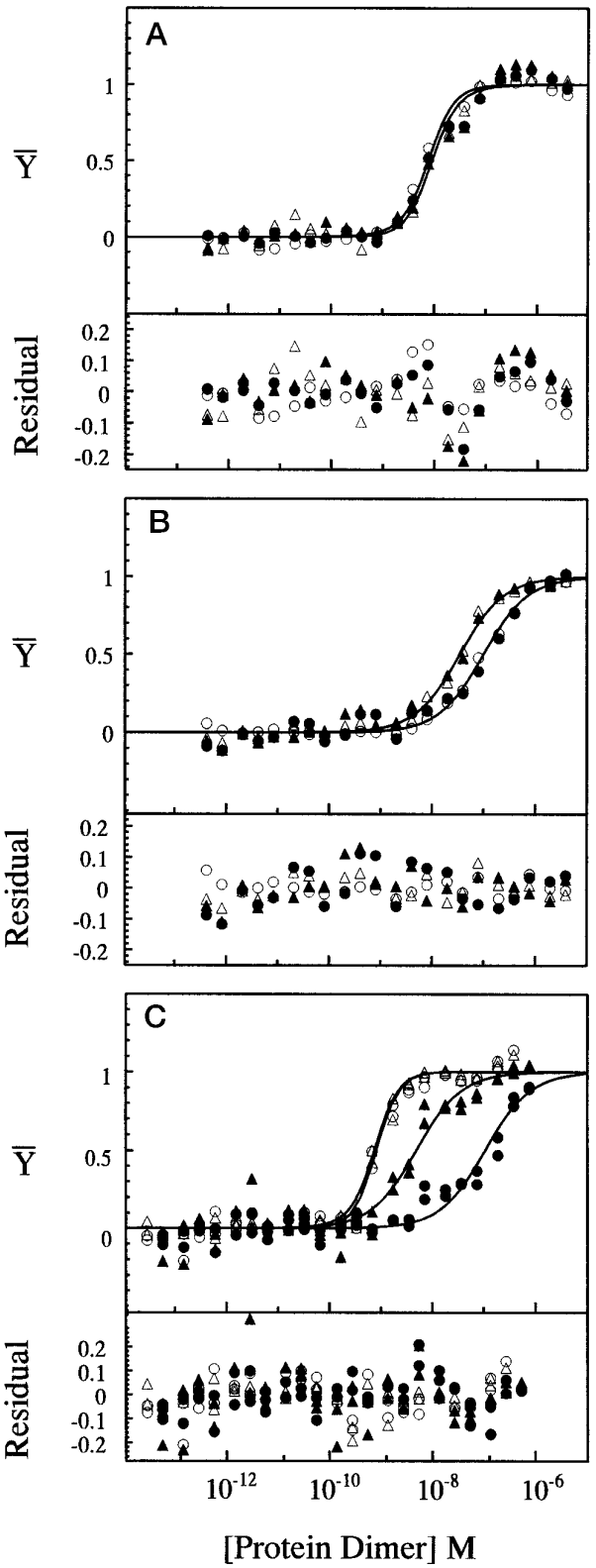

FIG. 4. **Binding of $DctD_2$ to $B_{G\rightarrow C}$ and $B_{G\rightarrow C}$+5 templates, and of $(DctD_{\Delta(1-142)})_2$ to WT and +5 templates.** *Circles*, site A; *triangles*, site B. *A*, template $B_{G\rightarrow C}$; note that the A and $B_{G\rightarrow C}$ site isotherms overlap and require slightly higher protein concentrations for occupancy than was true for WT template in Fig. 3*A*. *Open* and *closed symbols* represent two separate experiments. *B*, template $B_{G\rightarrow C}$ with 5-base pair insertion; occupancy at the $B_{G\rightarrow C}$ site requires more protein than the wild type site B (see Fig. 3, *B* and *C*), while occupancy at the A site is identical when separated by the 5-base pair insertion from site $B_{G\rightarrow C}$ or site B (see Fig. 3*B*). *Open* and *closed symbols* represent two separate experiments. *C*, both the wild type template (*open symbols*, two experiments) and the template with wild type sites separated by a 5-base pair insertion (*closed symbols*, two experiments) are shown, titrated with $(DctD_{\Delta(1-142)})_2$. In comparing these data with that of Fig. 3, note that occupancy on the 5-base pair insertion template is identical with that of $DctD_2$; however, occupancy of the wild type UAS configuration requires less $(DctD_{\Delta(1-142)})_2$ than $DctD_2$, indicating higher cooperativity for the deletion mutant.

More importantly, they strongly suggest that a cooperative protein/DNA-protein/DNA interaction is involved in binding of $DctD_2$ to the *dctA* UAS, and provide an estimate of this cooperativity. This cooperativity in effect allows occupancy at each site to be roughly equal at a given concentration of $DctD_2$. Finally, the results show that the truncated, constitutively active mutant $DctD_{\Delta(1-142)}$ binds to the *dctA* UAS with greater cooperativity than does the wild type protein.

Concluding that cooperativity contributes to binding of $DctD_2$ to the *dctA* UAS is based in part on the observation that DctD was apparently a dimer in solution at concentrations as low as 2 nM total monomer, and that it did not show any evidence of further multimerization up to concentrations of 2 μM total monomer. Since the binding isotherm changed most between 1 nM and 10 nM $DctD_2$, dimerization can probably be ruled out as a contributing factor for binding to the *dctA* UAS. This conclusion has to be tempered with the realization that elution volumes for small zone gel filtration experiments are not always correlated with molecular weight (36). It was also apparent from the DNase I titrations that $DctD_2$ is capable of binding independently to single sites. The fact that the single site binding data for both sites A and B are described well by the Langmuir binding polynomial also suggests that the oligomeric state of DctD is stable.

We analyzed binding of $DctD_2$ to the *dctA* UAS with a simple two-site, cooperative model, as previously developed for bacteriophage λ repressor cI (37). Under the conditions tested and so modeled, $DctD_2$ binds to the A and B sites of the *dctA* UAS with respective intrinsic affinities of -9.4 ± 0.3 kcal/mol and -11.2 ± 0.2 kcal/mol, with a cooperativity free energy of -2.5 ± 0.5 kcal/mol (75-fold increased binding). The separate analyses of all five UAS templates are internally consistent with this model. First, the Δ*A* and +5 templates give the same estimate for ΔG_B, and the insertion mutation does so for ΔG_A in both wild type and site $B_{G\rightarrow C}$ attenuation templates. Second, the attenuation mutant appears to only change the intrinsic binding energy for site B. In this analysis, it is possible that we have underestimated the intrinsic binding free energies, as we do not know the fraction of $DctD_2$ that is competent to bind to DNA. Our estimate of cooperativity is not affected by assuming that all of $DctD_2$ is active for DNA binding, provided that the true fraction of active protein is uniformly competent to participate in cooperative interactions.

The above analysis is crucially dependent upon the assumption that the 5-bp insertion mutation does not disturb intrinsic binding to site A, site B, or site $B_{G\rightarrow C}$. The importance of this assumption is indicated by the inability of the regression analyses to determine the same intrinsic binding and cooperativity estimates when only data from the wild type or attenuated site B DNA templates are considered. This means that the shape of the isotherms obtained for these UAS elements are not able to verify the cooperativity indicated by the global analyses. Instead, invoking cooperativity is entirely dependent upon including the data from the 5-bp insertion templates, which provide the information about intrinsic binding to site A in the absence of cooperativity. The fact that deleting site A yielded a similar estimate for intrinsic binding to site B provides some confidence for the assumption; however, the deletion template is itself subject to the assumption that its mutation does not affect intrinsic binding to site B. Studies of λ cI binding to O_R1

TABLE III

Microscopic Gibbs free energies of DctDΔ(1–142)$_2$-UAS interactions resolved by footprint titration of wild type and mutant UAS elements

Free energies (in kilocalories per mole) are presented with 67% confidence intervals according the two-site cooperativity model. Values in parentheses were fixed for that analysis. WT, wild type.

UAS elements	ΔG_A	ΔG_B	ΔG_{AB}	σ[a]
WT, +5	−9.4 ± 0.6	−11.1 ± 0.3	−3.8 ± 0.6	0.053
WT[b]	−10.1 (−11.5, −4.3)[b]	−10.4 (−11.5, −7.6)[b]	−3.8 (−12.5, −1.7)[b]	0.047
WT	−10.1 ± 1.0	−10.4 ± 1.0	(−3.8)	0.046
+5	−9.4 ± 0.4			0.047
+5		−11.2 ± 0.3		0.069

[a] Square root of the variance of the fitted curves.

[b] Although the least squares analysis converged on estimates for all three parameters, the confidence intervals were markedly broad and asymmetric.

have illustrated the importance of examining DNA binding interactions in the native context with flanking DNA present (38). If point mutants can be identified which effectively reduce the valency of the *dctA* UAS without disturbing binding to adjacent sites, then DNase I studies of them might address this problem.

Implicit in the above assumption is the general presumption that the intrinsic and cooperative energies for $DctD_2$ binding to the *dctA* UAS are unlinked, allowing them to be studied in each other's absence. This simplifying assumption has certainly been questioned for other systems (39–42). For example, non-additivity of thermodynamic energies (40, 41) and direct evidence of conformational changes in λ O_R upon binding of cI (42) imply a role for DNA sequence-dependent conformational changes in the mechanisms of both intrinsic and cooperative binding of cI to O_R. We observed no evidence of hypersensitivity within or between the DctD binding sites that might indicate such conformational changes. Further evidence that is consistent with intrinsic binding and cooperativity being unlinked in the *dct* system was provided by comparing data for the wild type and $B_{G\rightarrow C}$ mutation templates. The global and individual analyses for these data indicated that at the 67% confidence level, the point mutation reduced DctD's intrinsic affinity for mutant site B but left unchanged its affinity for site A and the apparent cooperativity between the two protein-DNA complexes.

There are several possible functions for a cooperative DctD-UAS interaction. First, DctD may have a dual function as an activator and as an autorepressor, repressing the transcription of *dctBD*. Occupancy of the UAS would be greater than 95% at a concentration of 10 nM, allowing repression at presumed minimal cellular concentrations of DctD. Although little is known about transcription of *dctBD*, the position of the UAS is such that it could block binding of RNA polymerase at the *dctBD* promoter. Also, strong binding of DctD to the *dctA* UAS even when DctD is in an inactive form may insulate the *dctA* promoter from spurious activation by other σ^{54}-dependent transcriptional activators (43). A third possible function of cooperativity is that $DctD_2$ may need to be in an oligomeric form to be transcriptionally active. This has been suggested for the similar two-component transcriptional activator protein, NtrC (28, 29), which has also been shown to bind cooperatively to the *glnA* UAS (26–28). It has been previously shown that $DctD_{\Delta(1-142)}$ has an ATPase activity (19). ATP hydrolysis was only seen at high protein concentrations and was increased in the presence of DNA. These observations are consistent with the active form of the protein being a higher oligomeric form.

One of the more interesting observations of these studies is that $DctD_{\Delta(1-142)}$ showed increased cooperativity relative to the transcriptionally inactive form. Such an increase in cooperativity may allow the active form of DctD to displace the inactive form from the *dctA* UAS. Alternatively, this additional interaction may be responsible for actually converting the inactive form to the active form. There may thus be two mechanisms mediating cooperativity in DctD, one detected in transcriptionally inactive protein, and the other appearing in transcriptionally active protein. $DctD_{\Delta(1-142)}$ may present only the latter, or both of these activities. If $DctD_{\Delta(1-142)}$ truly represents the active state typical of phosphorylated DctD, then the amino-terminal domain would not be needed for such cooperativity. However, an artifactual protein-protein interaction may have been caused by deleting the amino-terminal domain from DctD in making $DctD_{\Delta(1-142)}$. The increased cooperativity of $DctD_{\Delta(1-142)}$ is formally similar to the observation that cooperativity is increased in NtrC when it is phosphorylated (26–28). In that case, the increase is proposed to be mediated by properties of the phosphorylated amino-terminal domain of NtrC (44), and/or its central domain (27). In the latter report, based on DNase I footprint data, the authors also suggest that binding of ATP to the NtrC central domain influences cooperativity by 2-fold. While that might be true, estimating cooperativity effects of less than 3–4-fold may well be meaningless given the difficulty inherent to precise measurement of apparent constants (33).

It is also worth noting that the previous studies of *E. coli* and *S. typhimurium* NtrC that first demonstrated cooperative binding by a σ^{54}-dependent transcription activator utilized filter binding (26) and gel shift assays (28). Both studies reported about a 20-fold cooperative binding by NtrC, which was observed to increase upon phosphorylation of NtrC; however, the estimates of the increase in cooperativity due to phosphorylation were 50,000-fold *versus* 12-fold. While several features of the studies differed, the magnitude of this discrepancy remains to be explained. DNase I has a distinct advantage over other methods of studying multiple site DNA-protein interactions because occupancy at each site can be monitored separately in the same experiment. This is particularly important when it is believed that the two sites have different intrinsic binding affinities because it may be difficult, or even impossible, to distinguish between site heterogeneity and cooperativity using filter binding (31) or gel shift (45, 46) approaches. In a more recent DNase I footprint study of *E. coli* NtrC binding to the *glnA* UAS region (27), 20-fold cooperativity for binding of unphosphorylated protein was estimated to increase 12-fold upon phosphorylation. These values are most similar to those reported for *Salmonella* NtrC (28).

Acknowledgments—We thank Donald Senear, David Bains, David Burz and Gary Ackers for helpful discussions, especially regarding the statistical analysis of DNase I footprint data.

REFERENCES

1. Ronson, C. W., Lyttleton, P., and Robertson, J. G. (1981) *Proc. Natl. Acad. Sci. U. S. A.* **78,** 4284–4288
2. Finan, T. M., Oresnik, I., and Bottacin, A. (1988) *J. Bacteriol.* **170,** 3396–3403
3. Arwas, R., McKay, I. A., Rowney, F. R. P., Dilworth, M. J., and Glen, A. R. (1985) *J. Gen. Microbiol.* **131,** 2059–2066
4. Bolton, E., Higgisson, B., Harrington, A., and O'Gara, F. (1986) *Arch. Microbiol.* **144,** 142–146

5. Engelke, T., Jagadish, M. N., and Puhler, A. (1987) *J. Gen. Microbiol.* **133,** 3019–3029
6. Ronson, C. W., Astwood, P. M., Nixon, B. T., and Ausubel, F. W. (1987) *Nucleic Acids Res.* **15,** 7921–7934
7. Engelke, T., Jording, D., Kapp, D., and Puhler, A. (1989) *J. Bacteriol.* **171,** 5551–5560
8. Jiang, J., Gu, B., Albright, L. M., and Nixon, B. T. (1989) *J. Bacteriol.* **171,** 5244–5253
9. Watson, R. J. (1990) *Mol. Plant-Microbe Interact.* **3,** 174–181
10. Ronson, C. W., Nixon, B. T., Albright, L. M., and Ausubel, F. M. (1987) *J. Bacteriol.* **169,** 2424–2431
11. Ronson, C. W., and Astwood, P. M. (1985) in *Nitrogen Fixation Research Progress* (Evans, H. J., Bottomly, P. J., and Newton, W. E., eds) pp. 201–207, Martinus Niijhoff, Dordrecht, The Netherlands
12. Wang, Y. P., Birkinhead, K., Boesten, B., Manian, S., and O'Gara, F. (1989) *Gene* (*Amst.*) **85,** 135–144
13. Yarosh, O. K., Charles, T. C., and Finan, T. M. (1989) *Mol. Microbiol.* **3,** 813–823
14. Nixon, B. T., Ronson, C. W., and Ausubel, F. M., (1986) *Proc. Natl. Acad. Sci. U. S. A.* **83,** 7850–7854
15. Ronson, C. W., Nixon, B. T., and Ausubel, F. M. (1987) *Cell* **49,** 579–581
16. Volz, K. (1993) *Biochemistry* **32,** 11741–11753
17. Parkinson, J. S. (1993) *Cell* **73,** 857–871
18. Weiss, D. S., Batut, J., Klose, K. E., Keener, J., and Kustu, S. (1991) *Cell* **67,** 155–168
19. Lee, J. H., Scholl, D., Nixon, B. T., and Hoover, T. R. (1994) *J. Biol. Chem.* **269,** 20401–20409
20. Giblin L., Boesten B., Turk S., Hooykaas P., and O'Gara F. (1995) *FEMS Microbiol. Lett.* **126,** 25–30
21. Huala, E., and Ausubel, F. M. (1992) *J. Bacteriol.* **174,** 1428–1431
22. Gu., B., Lee, J.-H., Hoover, T. R., Scholl, D., and Nixon, B. T. (1994) *Mol. Microbiol.* **13,** 51–66
23. Lee, J. H., and Hoover, T. R. (1995) *Proc. Natl. Acad. Sci. U. S. A.* **92,** 9702–9706
24. Ledebur, H., Gu, B., Sodja, J., III, and Nixon, B. T. (1990) *J. Bacteriol.* **172,** 3888–3897
25. Ledebur, H., and Nixon, B. T. (1992) *Mol. Microbiol.* **6,** 3479–3492
26. Weiss, V., Claverie-Martin, F., and Magasanik, B. (1992) *Proc. Natl. Acad. Sci. U. S. A.* **89,** 5088–5092
27. Chen, P., and Reitzer, L. J. (1995) *J. Bacteriol.* **177,** 2490–2496
28. Porter, S. C., North, A. K., Wedel, A. B., and Kustu, S. (1993) *Genes Dev.* **7,** 2258–2273
29. Mettke, I., Fiedler, U., and Weiss, V. (1995) *J. Bacteriol.* **177,** 5056–5061
30. Maniatis, T., Fritsch, E. F., and Sambrook, J. (1982) *Molecular Cloning: A Laboratory Manual*, pp. 86–91, 454, Cold Spring Harbor Laboratory, Cold Spring Harbor, NY
31. Senear, D. F., Brenowitz, M., Shea, M. A., and Ackers, G. K. (1986) *Biochemistry* **25,** 7344–7354
32. Koblan, K. S., Bain, D. L., Beckett, D., Shea, M. A., and Ackers, G. K. (1992) *Methods Enzymol.* **210,** 405–426
33. Senear, D. F., and Bolen, D. W. (1992) *Methods Enzymol.* **210,** 463–481
34. Johnson, M. L., and Faunt, L. M. (1992) *Methods Enzymol.* **210,** 1–37
35. Beechem, J. M. (1992) *Methods Enzymol.* **210,** 37–54
36. Ackers, G. K. (1970) *Adv. Protein Chem.* **24,** 343–446
37. Ackers, G. K., Johnson, A. D., and Shea, M. A. (1982) *Proc. Natl. Acad. Sci. U. S. A.* **79,** 1129–1133
38. Brenowitz, M., Senear, D. F., and Ackers, G. K. (1989) *Nucleic Acids Res.* **17,** 3747–3755
39. Saroff, H. A. (1993) *Biopolymers* **33,** 1327–1336
40. Senear, D. F., Laue, T. M., Ross, J. B. A., Waxman, E., Eaton, S., and Rusinova, E. (1993) *Biochemistry* **32,** 6179–6189
41. Merabet, E., and Ackers, G. K. (1995) *Biochemistry* **34,** 8554–8563
42. Strahs, D., and Brenowitz, M. (1994) *J. Mol. Biol.* **244,** 494–510
43. Labes, M., and Finan, T. M. (1993) *J. Bacteriol.* **175,** 2674–81
44. Fiedler, U., and Weiss, V. (1995) *EMBO J.* **14,** 3696–3705
45. Senear, D. F., and Brenowitz, M. (1991) *J. Biol. Chem.* **266,** 13661–13671
46. Senear, D. F., Dalma-Weiszhausz, D. D., and Brenowitz, M. (1993) *Electrophoresis* **14,** 704–712